

Reduction of Magnetic Field from Receiving Side by Separated Coil in Contactless Charging Systems for Moving Electric Vehicle

S. Aoki, F. Sato^{**}, S. Miyahara^{*}, H. Matsuki^{*}, and T. Takura^{***}

Graduate School of Engineering, Tohoku Univ., 6-6-05 Aramaki-aza Aoba, Aoba-ku, Sendai, Miyagi 980-8579 Japan

^{*} Graduate School of Biomedical Engineering, Tohoku Univ., 6-6-05 Aramaki-aza Aoba, Aoba-ku, Sendai, Miyagi 980-8579 Japan

^{**} School of Engineering, Tohoku Gakuin Univ., 1-13-1 Chuo, Tagajo, Miyagi 985-8537 Japan

^{***} School of Engineering, Tohoku Institute of Tech., 35-1 Kasumi-cho, Taihaku-ku, Sendai, Miyagi 982-0831 Japan

Two main obstacles to the wider adoption of electric vehicles are short cruising distances and long charging times. We have proposed contactless charging systems for moving electric vehicles utilizing electromagnetic induction. A problem in these systems is high level magnetic field spreading far and wide from feeding and receiving coils, which can affect electronics and human health. In our previous work, we proposed a new feeding coil shape (multipolar coil) that reduced magnetic field at a distance by over 90%. In this paper, to reduce magnetic field from the receiving coil, we newly propose a separated receiving coil and compare it with a conventional spiral receiving coil. Simulations and power transmission experiments revealed that the separated coil greatly reduced the magnetic field far from the coil and achieved high power transmission efficiency of over 80%.

Key words: Contactless charging system, Electric vehicle, Magnetic fields

1. Introduction

1.1 Contactless Charging Systems for Moving Electric Vehicles

Recently, electric vehicles (EVs) have attracted attention as environmental awareness has grown. Current EVs have problems such as short cruising distances and long charging times. These problems have prevented EVs from becoming more widespread.

To solve these problems, we have proposed contactless charging systems for moving EVs and have performed various investigations^{1,2)}. These systems are able to transfer power from feeding coils in the road to a receiving coil on the underside of the EV by utilizing electromagnetic induction, which makes it possible to increase cruising distances without relying on battery capacity. Figure 1 shows a schematic diagram of a contactless charging system for moving EVs. These systems consist of an AC source, compensation circuits, feeding coils, a receiving coil, matching circuits, rectifiers, and a load (a battery or motor). The shape of the feeding coils is different from that of the receiving coil, and the size is larger in order to deliver stable magnetic coupling and transmission power³⁾.

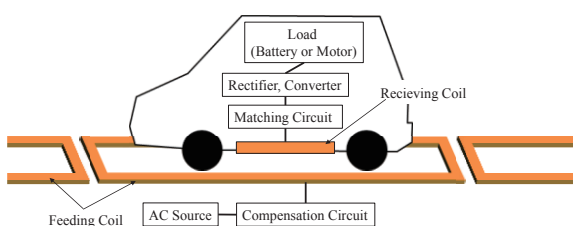


Fig. 1 Contactless charging systems for moving EVs

1.2 Electromagnetic Induction

Figure 2 shows a circuit diagram of contactless charging systems that utilize electromagnetic induction. In this figure, the resistances r_1 and r_2 are wire-wound resistors, P_{in} is input power to inverter, P_{out} is load power and the capacitances connected in series and parallel with the receiving coil are load matching capacitances. These capacitances enable power to be transmitted at maximum efficiency¹⁾. The maximum efficiency, η_{max} , is determined by the coupling factor k and the quality factors Q_1 and Q_2 of the coils. Using these parameters, the performance factor α is defined as follows¹⁾.

$$\alpha = k^2 Q_1 Q_2 \quad (1)$$

By using α , η_{max} can be expressed as¹⁾

$$\eta_{max} = \frac{1}{1 + \frac{2}{\alpha}(1 + \sqrt{1 + \alpha})} \quad (2)$$

The values of the load matching capacitances C_{2s} and C_{2p} can be written as¹⁾

$$C_{2s} = \frac{1}{\omega r_2 \left(Q_2 - \frac{R}{r_2} \sqrt{1 + \alpha} - (1 + \alpha) \right)} \quad (3)$$

$$C_{2p} = \frac{1}{\omega R \sqrt{\frac{R}{r_2} \sqrt{1 + \alpha} - 1}} \quad (4)$$

Figure 3 shows the relationship between η_{max} and the performance factor α . High transmission efficiency is required to achieve high α .

To compensate for the power factor, the value of the

capacitance connected in series with the feeding coil is given as follows:

$$C_1 = \frac{1}{\omega^2 L_1} \quad (5)$$

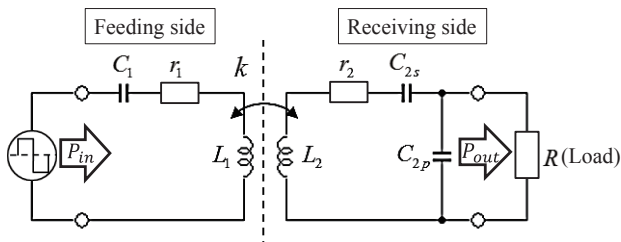


Fig. 2 Circuit diagram for contactless charging systems utilizing electromagnetic induction

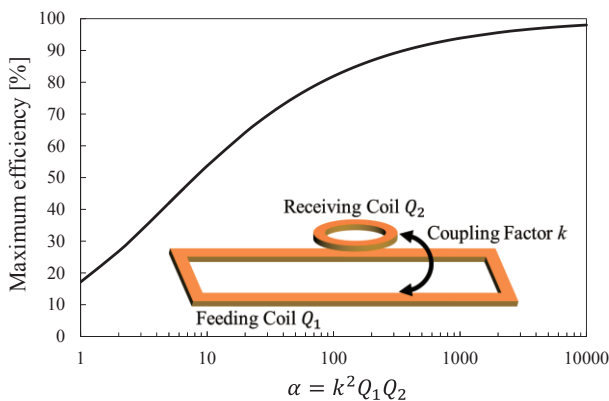


Fig. 3 Relation between α and maximum efficiency

1.3. Magnetic Field from Feeding and Receiving Coils

As shown in Fig. 1, the feeding coils are larger than the receiving coil in order to ensure stable magnetic coupling and to supply stable power along the direction of travel³⁾. The size of the feeding coils in the direction of travel is 5 to 10 m. Hence, the magnetic coupling factor, k , is assumed to be less than 0.1, meaning that high-level magnetic fields are generated from the feeding and receiving coils. The magnetic field can affect electronics and human health to a distant place. It is therefore necessary to reduce the magnetic field from these coils. Many studies have investigated reduction of magnetic field from contactless charging systems^{5),6)}.

In previous work, we proposed a new shape of feeding coil (multipolar coil) which is able to reduce the magnetic field at a distance by over 90% compared with that of conventional rectangular coils⁷⁾. The multipolar coil consists of a feeding loop at the center of the coil and two loops for offsetting the magnetic field on both sides of the feeding loop as shown in Fig. 4. The loops for offsetting the magnetic field are excited in the opposite phase to

the feeding loop in order to cancel out the magnetic field from the feeding loop. When the multipolar coil is used, the majority of the magnetic field from the combined feeding and receiving coil system is generated from the receiving coil. It is therefore necessary to reduce the magnetic field from the receiving coil in order to reduce the magnetic field from the overall system. In this article, we propose a new shape of receiving coil with the aim of reducing magnetic field from the receiving coil and we compare the proposed coil with a conventional spiral coil.

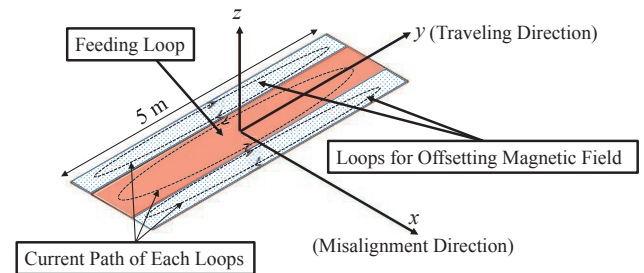


Fig. 4 Multipolar coil for reducing leakage magnetic field from the feeding coil

2. Separated Coil

2.1. Proposal of Separated Coil

We propose a new shape of coil which we call the separated coil. Figure 5 shows the structure of the separated coil. In this coil, the cross coil which has been proposed for contactless charging systems^{8),9)} is split into two coils that are connected differentially. By using this configuration, the magnetic field from both coils is canceled out, reducing the magnetic field at a distance. A high coupling factor between the feeding and receiving coils can be ensured by adjusting the spacing between both coils. In this study, we define the distance between the two coils as the parameter “*Space*”.

Figure 6 shows the configuration and size of the separated coil and spiral coil that were used as receiving coils in this study. The litz wire used in both coils consists of 2232 strands of 0.1 mm thick wire, and a Mn-Zn ferrite plate with a relative permeability is 2400 is placed inside the separated coil and behind the spiral coil in order to increase the inductance.

Table 1 shows the electrical properties of the separated coil and spiral coil at 100 kHz as measured with an LCR meter (E4980A, Agilent Co.) when *Space* was 0 mm, 200 mm, and 500 mm. As can be seen in the table, a high quality factor Q was confirmed as the *Space* parameter was increased because this decreased the mutual inductance and increased the

self-inductance.

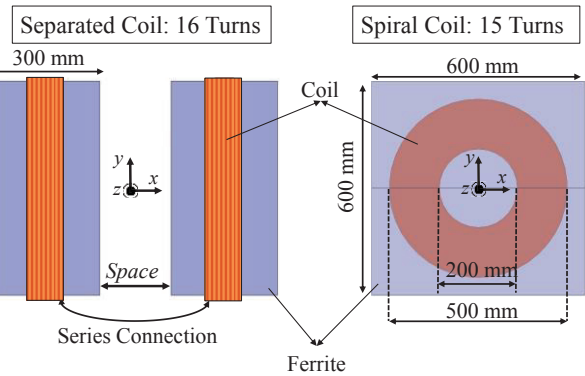
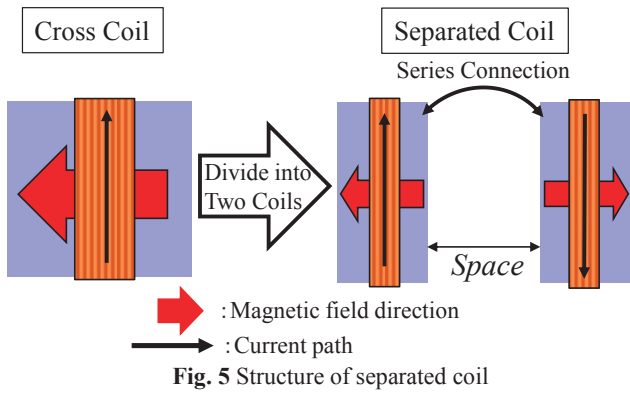


Fig. 6 Configuration and size of separated coil and spiral coil

Table 1 Electrical properties of the receiving coils (frequency: 100 kHz)

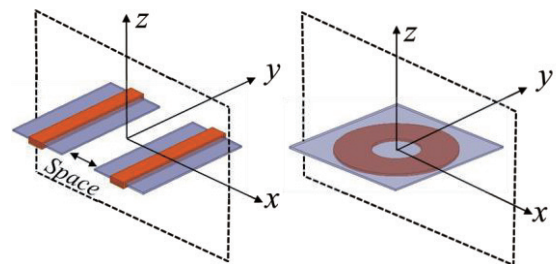
Coil	Turns	Space [mm]	L [μH]	r [$\text{m}\Omega$]	Q
Separated Coil	16	0	148	88.0	1059
		200	161	93.0	1087
		500	165	93.0	1112
Spiral Coil	15		152	113.7	840

2.2. Comparison of Magnetic Field Generated from Receiving Coils

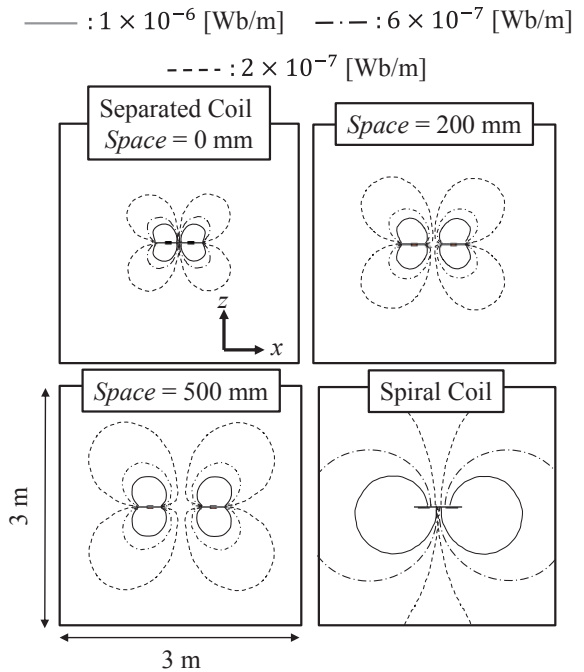
First, in order to indicate magnetic field structures of separated coil and spiral coil, we analyzed flux lines generated from each coils. Figure 7-(a) shows the simulation models and analysis plane (x - z plane). Figure 7-(b) shows the analysis results. The excitation condition is a current of 1 A. In Fig.7 (b), we used Maxwell®2D electromagnetic field analysis software (ANSYS Co.) to analyze the flux lines and the value of vector potential. As shown in the Fig. 7-(b), the separated coils exhibit a 4-pole structure and their flux lines concentrate in near the

coils compared with that of the spiral coil. As the *Space* parameter increases, the magnetic flux near the coil increases without the 4-pole structure changing. This characteristic makes it possible to reduce the magnetic field far from the coil and to increase interlinkage flux through the feeding coil and the coupling factor between the feeding coil and receiving coil.

Next, Fig. 8 shows comparison results for magnetic flux density at 10 m from the center of the coil on the x , y , and z axes (as shown in Fig. 8-(a)). In Figure 8-(b), the value of flux density was calculated by Maxwell®3D electromagnetic field analysis software (ANSYS CO.) The excitation condition is a current of 1 A and a frequency of 100 kHz. In Fig.8-(b), the magnetic flux density far from the separated coils smaller than that from the spiral coil. The magnetic flux density from the separated coil with *Space* = 0 mm was lower by 73% on the x -axis, 86% on y -axis, and 93% on the z -axis. This shows that the separated coil reduces the magnetic field at a distance from the receiving coil.



(a) Simulation models and analysis plane



(b) Magnetic flux lines on the x - z plane

Fig. 7 Simulation models and flux lines on the x - z plane

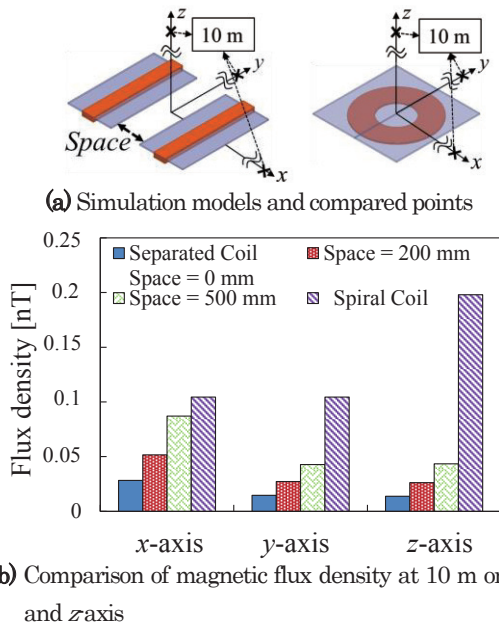


Fig. 8 Simulation models and comparison of magnetic flux density at 10 m on the x , y , and z axis

2.3 Coupling Coefficient between the Feeding and Receiving Coils

We measured the coupling coefficient between the feeding and receiving coils when the separated coil ($Space = 0$ mm, 200 mm, and 500 mm) and spiral coil were used as the receiving coil. Figure 9 shows the configuration of the measurement model. The feeding coil is a multipolar coil (length: 5 m; width: 1.6 m; number of loops: 1 turn). The gap between the feeding and receiving coils was set to 170 mm.

Figure 10 shows coupling factor versus location of the receiving coil along the direction of travel. The measurement results indicate that the coupling coefficient increased with increasing $Space$. This is due to an increase in the interlinkage flux as mentioned in Section 2.2, and also due to the change in relative distance between the feeding and receiving coils. The coupling coefficient was 0.035 for $Space = 200$ mm, which is comparable to the value for the spiral coil, and was 0.06 for $Space = 500$ mm. This shows that it is possible to achieve high transmission efficiency while reducing the magnetic field by using a separated coil as the receiving coil.

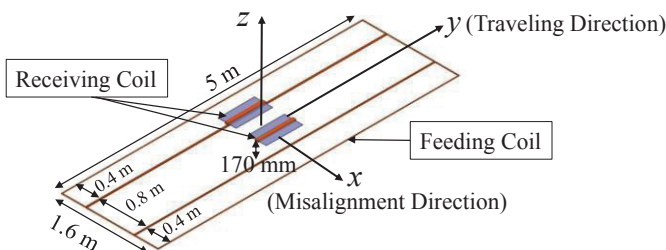


Fig. 9 Feeding and receiving coils

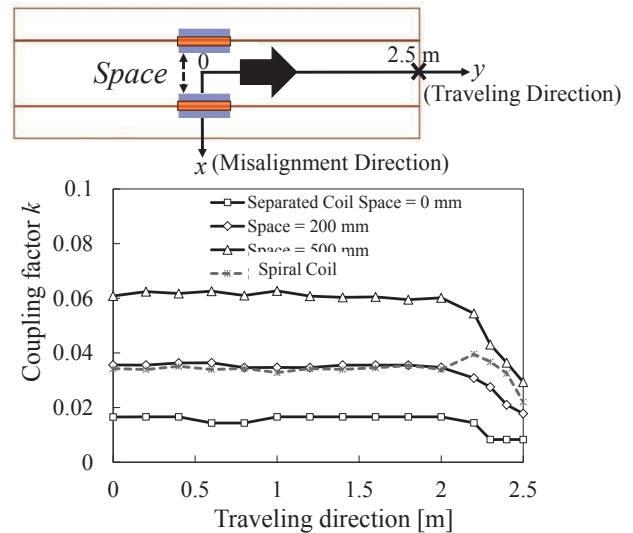


Fig. 10 Coupling factor along the direction of travel

3. Transmission Experiment and Evaluation of Magnetic Field

3.1 Transmission Experiment

We conducted transmission experiments using separated coils ($Space = 0$ mm, 200 mm, and 500 mm) and a spiral coil as the receiving coil, and measured the transmission efficiency.

The input power to the inverter was fixed at 100 W and the frequency was 100 kHz. Table 2 shows the electrical properties of the feeding coil (multipolar coil). A resistance load (10Ω) was connected after the secondary load matching capacitances (Fig. 2).

Figure 11 shows the transmission efficiency along the direction of travel. The transmission efficiency at the center of the feeding coil was 82.1% when a separated coil with $Space = 200$ mm was used, and was 88.1% for $Space = 500$ mm. We thus confirmed that a contactless charging system with a high transmission efficiency can be constructed by using a separated coil as the receiving coil.

Table 2 Electrical properties of the feeding coil (frequency: 100 kHz)

Coil	Turns of each loop	L [μ H]	r [$m\Omega$]	Q
Multipolar Coil	1	46	88.1	330

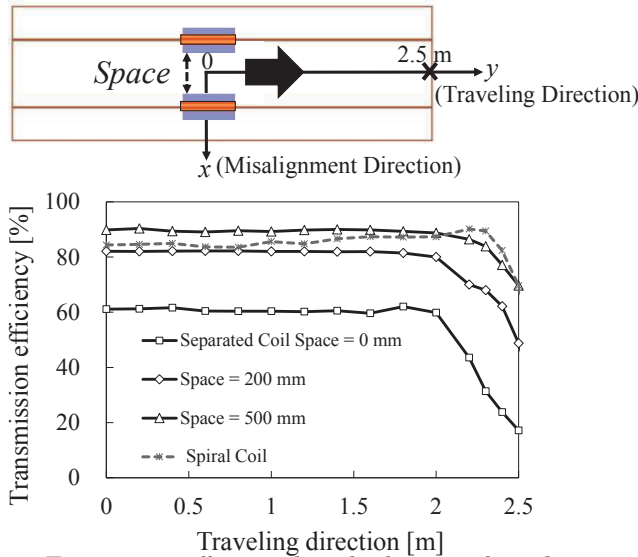


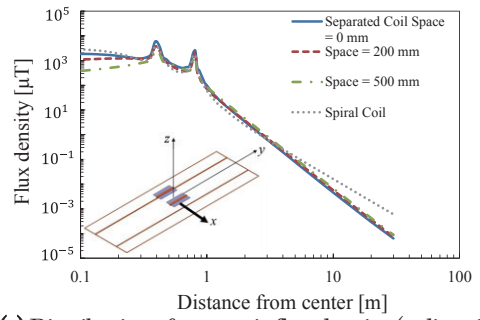
Fig. 11 Transmission efficiency along the direction of travel

3.2 Evaluation Magnetic Field from Feeding and Receiving Coils during Transmission

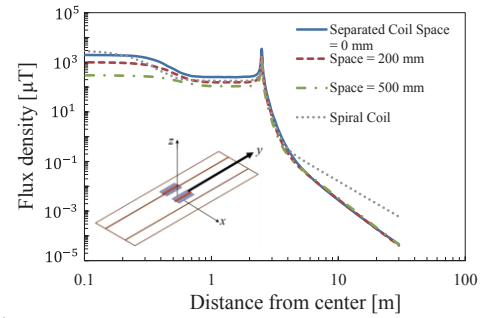
We analyzed the magnetic field surrounding coils during transmission and evaluated the separated coil compared to a spiral coil. Table 3 shows the estimated current values when the load power is 20 kW (by means of circuit analysis). We also analyzed the magnetic field from the feeding and receiving coils by Maxwell® 3D in terms of current values. Figure 12 shows the distribution of magnetic flux density from feeding and receiving coil. Figure 12-(a) is the distribution in the x -direction, (b) is in the y -direction and (c) is in the z -direction. As shown in Figure 12, flux density when the separated coil was used as the receiving coil is lower than spiral coil as it goes away farther from center of coil. And Figure 13-(b) shows the result of comparing the magnetic flux density at 10 m from the center of the coil on the x , y , and z axes (as shown in Figure 13-(a)). The leakage magnetic field was reduced by 64% on the x -axis, 81% on the y -axis and 90% on the z -axis compared to using a spiral coil when the separated coil with $Space = 200$ mm was used as the receiving coil.

Table 3 Coil current (20 kW class)

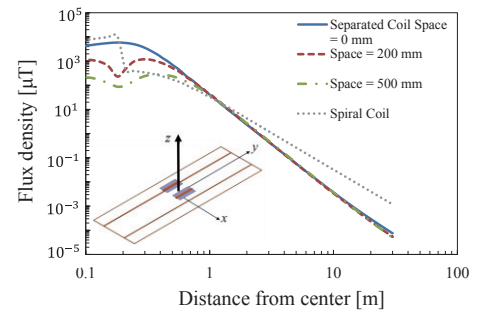
Receiving Coil	Space [mm]	$I_{Feeding_coil}$ [A]	$I_{Receiving_coil}$ [A]
Separated Coil	0	171	159
	200	103	106
	500	72	76
Spiral Coil		118	99



(a) Distribution of magnetic flux density (x -direction)

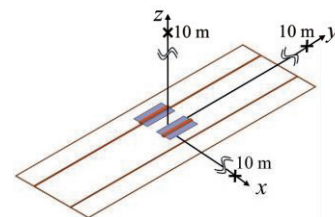


(b) Distribution of magnetic flux density (y -direction)

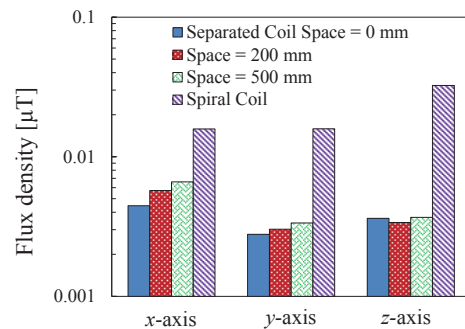


(c) Distribution of magnetic flux density (z -direction)

Fig. 12 Distribution of magnetic flux density from



(a) Simulation model and compared points



(b) Comparison of magnetic flux density (at 10 m from center of feeding coil)

Fig.13 Comparison of magnetic flux density

4. Summary

In this study, we examined the magnetic field from the receiving coil in contactless charging systems for moving EVs. This paper newly introduced the concept of the separated coil for use as the receiving coil, and compared it with a conventional spiral coil

The results of analyses and experiment showed that the magnetic field far from the coil can be reduced by approximately 90% and high transmission efficiency can be obtained by means of adjusting the *Space* parameter.

In future work, it is necessary to identify the magnetic field when the receiving coil is fitted to an EV and to reduce further magnetic field by using magnetic shielding such as aluminum sheet.

References

- 1) T. Takura, A. Aruga, F. Sato, T. Sato, H. Matsuki
EVTec and APE Japan Conference Proceedings 20144028 pp.1-7 (2014)
- 2) T.Misawa, T.takura, F.Sato, and H.Matsuki : *IEICE Technical Report WPT2012-33*, pp13-18 (2012) (in Japanese)
- 3) N.Aruga, Y.Ota, Y.Imamura, S.Sato, and H. Matsuki: *J.Magn.Soc.Jpn.*, **39**, No.3, pp.121-125 (2015)
- 4) T.Takura, Y.Ota, K.Kato, F.Sato, and H.Matsuki
J. Magn. Soc. Jpn., **35**,pp. 132-135, (2011)
- 5) J.Shin, B.Song, S. Chung, Y.Kim, G.Jung and S.Jeon : *IEEE Wireless Power Transfer (WPT)*, pp. 56-59 (2013)
- 6) D.Narita, T.Imura, H.Fujimoto, Y.Hori: *IEICE Technical Report WPT2014-31*, pp39-44 (2014) (in Japanese)
- 7) S.Aoki, F.Sato, S.Miyahara, H.Matsuki, and T.Takura: *IEICE Technical Report WPT2015-28*, pp43-48 (2015) (in Japanese)
- 8) Y.Kaneko, N.Ehara, T.Iwata, S.Abe, T.Yasuda, K.Ida: *IEEE Trans. IA*, Vol.**130**,No.6,pp.734-741 (2010) (in Japanese)
- 9) H.Yamaguchi, T.Takura, F.Sato, and H.Matsuki: *J.Magn.Soc.Jpn.*, **38**, No.2-1 pp.33-36 (2014)

Received Oct. 16, 2015; Revised Nov. 24, 2015; Accepted Dec. 4, 2015